

# Competition between electroconvection and Freedericksz distortions in nematics with slightly positive dielectric anisotropy

B. Dressel and W. Pesch

*Physikalisches Institut der Universität Bayreuth, D-95440 Bayreuth*

(Dated: February 14, 2003)

Planar electroconvection in nematic liquid crystals with positive dielectric anisotropy is theoretically studied for the first time in the nonlinear regime. The system is characterized by a competition between the non-equilibrium electroconvection instability and equilibrium Freedericksz distortions. Near a resulting multicritical bifurcation point a novel splay-roll instability and bistability between the convective and the homogeneous state occur.

PACS numbers: 61.30.Gd, 47.54.+r, 47.20.Lz

## I. INTRODUCTION

Electroconvection in nematic liquid crystals (nematics) is widely accepted as an excellent paradigm to study pattern forming instabilities in anisotropic systems [1–5]. Nematics are intrinsically anisotropic fluids with uniaxial symmetry. The preferred axis (the director  $\mathbf{n}$ ) corresponds to the mean orientation of their elongated molecules. Electroconvection (EC) occurs when a voltage above a critical threshold strength is applied across a thin layer of a nematic with nonvanishing electrical conductivity, which originates from impurities or from suitable doping. At convection onset typically a periodic array of convection rolls (stripes) is observed, which are associated with periodic director distortions perpendicular to the roll axes in the layer plane.

Besides the nonequilibrium EC instabilities alternatively equilibrium phase transitions (“Freedericksz transitions”) can be observed if electric (or magnetic) fields are applied to uniformly oriented nematics [2]. The resulting homogeneous director distortions, i.e. without spatial variations in the plane, are minimizers of the orientational elasticity potential characteristic for nematics [6]. The interplay between the periodic pattern-forming and the homogeneous modes is reflected in phenomena like “abnormal” rolls [7–10] or “dendritic growth” [11] which have no counterpart in the standard Rayleigh-Bénard convection. The bifurcation diagrams are organized by various multicritical points mainly in the nonlinear regime, such that the theoretical analysis as well as the experimental verification are quite demanding. In the present case EC is discussed in a system, where equilibrium and nonequilibrium phase transition and their competition are disentangled in a transparent manner, since a certain multicriticality is already seeded in the linear regime.

Our investigations concentrate on the familiar *planar* electroconvection. In the common capacitor-like configuration an ac-voltage  $V(t) = \sqrt{2} U \cos(\omega t)$  is applied in the  $z$ -direction between two transparent plates (in the  $x, y$ -plane), which confine a nematic layer. By a suitable surface treatment of the plates the director is orientated in a preferred direction (along  $\hat{\mathbf{x}}$ ) in the layer plane. The ef-

fective voltage amplitude  $U$  and the circular ac-frequency  $\omega$  serve as main control parameters. All material properties of nematics require a tensorial description. For instance the dielectricity tensor  $\epsilon$ , which expresses the electric displacement  $\mathbf{D} = \epsilon \cdot \epsilon_0 \mathbf{E}$  in terms of the electric field  $\mathbf{E}$ , has the representation  $\epsilon_{ij} = \epsilon_{\perp} \delta_{ij} + (\epsilon_{\parallel} - \epsilon_{\perp}) n_i n_j$  ( $i, j = x, y, z$ ), which reflects the uniaxial symmetry. Obviously  $\epsilon_{\perp}$  describes the dielectric response if  $\mathbf{E}$  is oriented perpendicular to  $\mathbf{n}$  while  $\epsilon_{\parallel}$  governs the case  $\mathbf{E} \parallel \mathbf{n}$ . For positive dielectric anisotropy  $\epsilon_a = \epsilon_{\parallel} - \epsilon_{\perp} > 0$ , the orientation of  $\mathbf{n}$  parallel to  $\mathbf{E}$  is energetically favored.

Historically, standard nematics, like 4-methoxybenzylidene-4'-n-butylaniline (MBBA) or a mixture, Merck Phase 5, with negative dielectric anisotropy  $\epsilon_a$  have played a major role in the investigation of EC, since there was hope to exploit them for designing liquid crystal displays [12]. For this reason most of the material parameters for those substances have been measured, which has allowed a quantitative comparison with theoretical calculations on EC [13]. For instance a spontaneously excited homogeneous *twist* mode, which corresponds to a rotation of the director in the plane of the nematic layer, has turned out to be essential for the interpretation of secondary instabilities in planar EC [14, 15]. A reverse sequence of bifurcations is typical for the *homeotropic* geometry (director orientation perpendicular to the confining plates, i.e. parallel to the applied electric field). First a primary Freedericksz transition takes place leading virtually about the center plane of the cell to a planar configuration, which at increasing voltages becomes convectionally unstable via a secondary bifurcation [16].

In this paper we study *planar* EC in nematics with *positive* dielectric anisotropy  $\epsilon_a > 0$ . This case, which has not attracted much interest so far, is in fact very convenient to investigate the competition between convective and homogeneous modes. While in the standard planar setup with  $\epsilon_a < 0$  the electric field  $\mathbf{E}$  ( $\parallel \hat{\mathbf{z}}$ ) is stabilizing, a destabilizing dielectric torque acts now on the director to align it with the field direction. However, an ensuing homogeneous distortion (Freedericksz transition) occurs only for an applied voltage amplitude  $U$  above a certain  $\omega$ -independent threshold  $U_F = \pi \sqrt{k_{11}/(\epsilon_a \epsilon_0)}$  (see

e.g. [17],  $k_{11}$  denotes the splay elastic constant), since opposing torques from the orientational elasticity have to be overcome. The Fredericksz transition can compete with the nonequilibrium EC instability of the basic state. EC becomes possible above a frequency dependent threshold voltage  $U_c(\omega)$ , which increases monotonously with  $\omega$  starting from  $U_c(0) \approx \pi^2 \sqrt{k_{11} \sigma_{\perp} / (\sigma_a \epsilon_{\perp} \epsilon_0)}$ . The material constants  $\sigma_{\perp}$  and  $\sigma_a$  are defined in analogy to  $\epsilon_{\perp}$ ,  $\epsilon_a$  via the components of the conductivity tensor  $\boldsymbol{\sigma} \equiv \sigma_{ij} = \sigma_{\perp} \delta_{ij} + \sigma_a n_i n_j$ . Note, that the ratio of  $\epsilon_{\perp}$ ,  $\sigma_{\perp}$  defines the charge relaxation time  $\tau_q = (\epsilon_{\perp} \epsilon_0) / \sigma_{\perp}$ , which serves as a our time scale in the sequel.

Inspection of the expressions for  $U_F$  and  $U_c(0)$  above reveals that the Fredericksz transition is in fact easily preempted by a primary EC instability at small  $\omega$  and not too large  $\epsilon_a$ . With increasing frequency  $U_c(\omega)$  approaches  $U_F$  from below until the curves cross at a codimension-2 (C2) point  $\omega = \omega_{C2}$ . The experimental studies of nematics with positive  $\epsilon_a$  have in fact exclusively concentrated on the *linear* threshold lines  $U_c$ ,  $U_F$  and the identification of  $\omega_{C2}$  (see e.g. [18, 19] and further references therein). Materials for a wider range of positive dielectric anisotropies  $\epsilon_a > 0$  were systematically synthesized by mixing MBBA with few weight percentages of suitable nematics (EBCA, MBCA) with large  $\epsilon_a \approx 20$ . Most material parameters (in particular the viscosities, see Sec. II below), which are needed for a precise comparison with the linear theory, have not been measured in these mixtures. However, the experimental  $U_c$ ,  $U_F$  threshold values compared well with theoretical calculations [18, 19] on the basis of a material parameter set, to which we refer as MBBA\* henceforth. In MBBA\* except  $\epsilon_a$  the material parameters of pure MBBA are used [20, 21]. The explicit bifurcation diagrams presented in this paper are calculated for MBBA\* with a representative medium value  $\epsilon_a = 0.1$ .

A simple consideration reveals that besides  $U_c$ ,  $U_F$  a further instability line in the nonlinear regime has to meet the C2 point. If the voltage amplitude  $U$  is lowered starting in the Fredericksz state for  $U \gg U_F$  and for  $\omega < \omega_{C2}$  one will hit for continuity reasons an upper transition line  $U_c^F(\omega) > U_F > U_c(\omega)$  to the convection state. All the transition lines are sketched in Fig. 1 to underline from beginning the generic framework for the bifurcation structure near  $\omega_{C2}$ , which is detailed below. A comprehensive analysis of the bifurcation diagram in the vicinity of  $\omega_{C2}$  has also revealed a rich variety of nonlinear bifurcation types. As an example for the complex structure of the multicritical point  $\omega_{C2}$  it will be demonstrated below that the bifurcation at the lines  $U_c$ ,  $U_F$  is supercritical, while it is subcritical and hysteretic at  $U_c^F$ . The resulting possibility of bistability between convection states and homogeneous Fredericksz distortions, has not been mentioned to our knowledge in the literature so far and might apply to other EC experiments as well.

The paper is organized as follows: First in section II we briefly present the fundamental equations as basis for our

theoretical calculations, also to fix our notations. Section III contains the analysis of the convection onset at the bifurcation lines  $U_c$  and  $U_c^F$ . In section IV the nonlinear bifurcation diagram for the substance MBBA\* is presented and discussed in detail. With some concluding remarks the paper will end in section V.

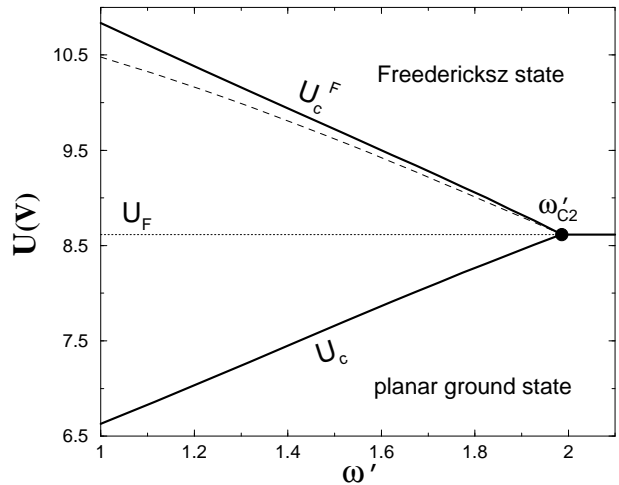


FIG. 1: Upper and lower convection onsets  $U_c$ ,  $U_c^F$  as function of the dimensionless frequency  $\omega' = \omega \tau_q$  together with the Fredericksz bifurcation line  $U_F = \pi \sqrt{k_{11} / (\epsilon_a \epsilon_0)}$  (solid lines) for MBBA\* with  $\epsilon_a = 0.1$ . The dashed line indicates a weakly-nonlinear approximation for  $U_c^F$  near the codimension-2 point  $\omega'_{C2}$  (see Sec. IIIB below).

## II. BASIC EQUATIONS

To explain the EC destabilization mechanism, which has been elucidated first by Carr and Helfrich [22, 23] a brief sketch of the standard nemato-hydrodynamic equations is sufficient [4, 24]. They describe the coupling between the director  $\mathbf{n}$ , the velocity  $\mathbf{v}$ , and the electric field  $\mathbf{E}$ , which derives as  $\mathbf{E} = -\nabla \phi$  from the electric potential  $\phi$ .

The important point is that in the presence of director distortions an electric current density  $\mathbf{j}_e = \nabla \cdot (\boldsymbol{\sigma} \cdot \mathbf{E})$  is inevitably associated with a charge density  $\rho_e = \nabla \cdot (\boldsymbol{\epsilon} \cdot \boldsymbol{\epsilon}_0 \mathbf{E})$  according to the continuity equation

$$\frac{d}{dt} \rho_e + \nabla \cdot \mathbf{j}_e = 0, \quad (1)$$

with  $d/dt = \partial_t + \mathbf{v} \cdot \nabla$  the substantial derivative. The bulk force  $\rho_e \mathbf{E}$  in the Navier-Stokes equation

$$\rho_m \frac{d}{dt} \mathbf{v} = \rho_e \mathbf{E} - \nabla p + \nabla \cdot \boldsymbol{\Sigma}, \quad (2)$$

with the pressure  $p$  and the mass density  $\rho_m$ , may then overcome the viscous stresses, to drive the velocity  $\mathbf{v}$ .

The fluid is assumed incompressible ( $\nabla \cdot \mathbf{v} = 0$ ).  $\Sigma$  denotes the stress-tensor with viscous and (almost negligible) elastic contributions. The explicit form of  $\Sigma$  (see e.g. [2, 4]), which goes up to quintic order in the components of  $\mathbf{v}$ ,  $\mathbf{n}$ , includes six (5 independent) Leslie shear viscosity coefficients  $\alpha_1, \dots, \alpha_6$  [25]. The familiar effective (Miesowicz) viscosities, which are determined by the relative orientations of  $\mathbf{n}$ ,  $\mathbf{v}$  and the gradients of  $\mathbf{v}$ , depend linearly on the  $\alpha_i$ . For instance the large shears  $\partial_x v_z$  and  $\partial_z v_x$  at a convection roll center in the planar case give rise to the Miesowicz viscosities  $\eta_1 = (\alpha_4 + \alpha_5 - \alpha_2)/2$  and  $\eta_2 = (\alpha_3 + \alpha_4 + \alpha_6)/2 < \eta_1$ , respectively.

Eventually the director dynamics is governed by:

$$\gamma_1 \mathbf{n} \times \frac{d}{dt} \mathbf{n} = \mathbf{n} \times (\mathbf{h}_{el} + \mathbf{h}_e + \mathbf{h}_v), \quad (3)$$

with  $\gamma_1 = \alpha_3 - \alpha_2$ . The restoring angular momenta in case of splay ( $k_{11}$ ), twist ( $k_{22}$ ) and bend ( $k_{33}$ ) director distortions are contained in the effective field  $\mathbf{h}_{el}$  derived from the Frank orientational elastic energy (see e.g. [2, 4, 6]). The dielectric and viscous torques  $\mathbf{h}_e$  and  $\mathbf{h}_v$ , respectively, are defined as:

$$\mathbf{h}_e = \epsilon_a \epsilon_0 (\mathbf{n} \cdot \mathbf{E}) \mathbf{E}, \quad \mathbf{h}_v = -\alpha_2 \mathbf{D} \cdot \mathbf{n} - \alpha_3 \mathbf{n} \cdot \mathbf{D}, \quad (4)$$

where the tensor  $\mathbf{D}$  ( $D_{ij} = \partial v_i / \partial x_j$ ) characterizes the velocity shear. For example the viscous torque contribution  $-\alpha_2 \partial_x v_z$  enhances the splay distortion of the director at the roll center. Equations (1), (2), (3) have to be solved with rigid boundary conditions  $\mathbf{v} = 0$ ,  $\mathbf{n} = \hat{\mathbf{x}}$  and  $\phi = \phi_0 = \mp \sqrt{2} U \cos(\omega t)$  at  $z = \pm d/2$  with  $d$  the cell thickness.

For a more compact notation we combine in the following all field variables in a symbolic vector  $\mathbf{V} = (\phi, \mathbf{n}, \mathbf{v})$ , so that the set of Eqs. (1), (2), (3) can be written in the symbolic form

$$\mathbf{B} \cdot \partial_t \mathbf{V} = \mathbf{L} \cdot \mathbf{V} + \mathbf{N}_2(\mathbf{V}, \mathbf{V}) + \mathbf{N}_3(\mathbf{V}, \mathbf{V}, \mathbf{V}) + \dots \quad (5)$$

The components of the vector operators  $\mathbf{N}_2, \mathbf{N}_3, \dots$  are quadratic, cubic, ... in  $\mathbf{V}$  and its spatial derivatives, whereas  $\mathbf{L}$  and  $\mathbf{B}$  represent matrix differential operators.

### III. ONSET OF CONVECTION

In the following the “lower” threshold curve  $U_c$  for the destabilization of the conductive ground state and the corresponding “upper” one,  $U_c^F$ , for the destabilization of the Freedericksz state, already shown in Fig. 1, are analyzed in detail.

#### A. Lower onset of convection at $U_c$

The calculation of the lower onset of convection  $U_c(\omega)$  requires a linear stability analysis of the planar ground-state  $\mathbf{V}_0 = (\phi_0, \mathbf{n}_0, \mathbf{v} = 0)$  with  $\mathbf{n}_0 = \hat{\mathbf{x}}$ . From Eq. (5)

we arrive by linearization of  $\mathbf{V} = \mathbf{V}_0 + \delta \mathbf{V}$  with respect to the convective perturbation  $\delta \mathbf{V}(\mathbf{r}, z, t)$  at the linear eigenvalue problem:  $\mathbf{B} \cdot \partial_t \delta \mathbf{V} = \mathbf{L} \cdot \delta \mathbf{V}$ . It is diagonalized by the ansatz  $\delta \mathbf{V}(\mathbf{r}, z, t) = e^{\lambda t} e^{i \mathbf{q} \cdot \mathbf{r}} \mathbf{V}(\mathbf{q}, z)$  with  $\mathbf{q} = (q, p)$ . The eigenvalue  $\lambda = \sigma + i\Omega$  with the maximal real part determines the growthrate  $\sigma(\mathbf{q}, \omega, U)$ . The condition  $\sigma = 0$  yields the neutral curve  $U_0(\mathbf{q}, \omega)$  with the minimum  $U_c(\omega) = U_0(\mathbf{q}_c, \omega)$  at  $\mathbf{q} = \mathbf{q}_c(\omega)$ . In the present case the bifurcation is stationary ( $\Omega = 0$ ) and we find typically normal rolls at threshold, i.e.  $\mathbf{q}_c = q_c \hat{\mathbf{x}}$ . Technically the eigenvalue problem is solved by a Galerkin method, where all fields are expanded with respect to the vertical coordinate  $z$  into a set of functions, that fulfill the (rigid) boundary conditions at the confining plates. The periodic time dependence of the eigenvector due to the applied ac-voltage is captured by Fourier series in time. The series expansions are appropriately truncated, such that the eigenvalue problem amounts to the diagonalization of a matrix acting in the space of the expansion coefficients. It turns out that the neutral curve is already very well described by keeping only the leading modes in  $z, t$ . One arrives thus at an one-mode approximation, which represents the dependence of the neutral curve on the material parameters in a particularly transparent manner:

$$U_0^2(q', \omega') = \frac{\pi^2 k_{11}}{\epsilon_{\perp} \epsilon_0} \frac{K(q') H(q', \omega')}{q'^2 A(q') + (\epsilon_a / \epsilon_{\perp}) B(q', \omega')}. \quad (6)$$

In Eq. (6) the abbreviations

$$K(q') = \frac{1 + (k_{33}/k_{11}) q'^2 + (H_x/H_F)^2}{1 + q'^2},$$

$$H(q', \omega') = \sigma(q')^2 + \omega'^2 \epsilon(q')^2,$$

$$\sigma(q') = q'^2 (1 + \sigma_a / \sigma_{\perp}) + 1, \quad \epsilon(q') = q'^2 (1 + \epsilon_a / \epsilon_{\perp}) + 1,$$

$$A(q') = \frac{a(q')}{\eta(q')} \equiv \frac{(\alpha_2 q'^2 - \alpha_3) \sigma(q') (\epsilon_a / \epsilon_{\perp} - \sigma_a / \sigma_{\perp})}{\eta_2 \lambda_1^4 + (\alpha_1 + \eta_1 + \eta_2) i_1 q'^2 + \eta_1 q'^4} I_h,$$

$$B(q', \omega') = \sigma(q') + \omega'^2 \epsilon(q')$$

are used. The numerical constants  $\lambda_1 = 1.50563$ ,  $i_1 = 1.24652$ ,  $I_h = 0.97267$  correspond to certain overlap integrals,  $q' = qd/\pi$  is the dimensionless wavenumber and  $\omega' = \omega \tau_q$  the ac-frequency in units of the charge relaxation time  $\tau_q$  [26]. For convenience we have included the effect of a planar stabilizing magnetic field  $\mathbf{H} = H_x \hat{\mathbf{x}}$  which is nondimensionalized in Eq. (6) with the help of the splay Freedericksz field  $H_F = (\pi/d) \sqrt{k_{11}/(\mu_0 \chi_a)}$ ;  $\chi_a > 0$  denotes the anisotropy of the magnetic susceptibility. According to the representative example of Fig. 2a for MBBA\* with  $\epsilon_a = 0.1$  the rigorous behavior of the critical voltage  $U_c(\omega') = \min_{q'} U_0(q', \omega')$  is already determined very satisfactorily from Eq. (6). The lines  $U_c$  and  $U_F$  cross in this case at the C2 point  $\omega'_{C2} = 1.99$ .

The  $\omega$ -dependence of the critical wavenumber  $q_c(\omega)$ , which in fact slightly decreases with increasing  $\omega'$  in Fig. 2b, might look unexpected, since for  $\epsilon_a < 0$  we are accustomed to a monotonous increase of  $q'_c(\omega')$  and a divergence also of  $U_c$  at the cut-off frequency  $\omega'_{cut} (\approx 2$

for MBBA with  $\epsilon_a = -0.53$  [4]). The rather smooth variations of  $U_c$ ,  $q_c$  with  $\omega$  can be understood by examining more closely the threshold formula Eq. (6). Stabilizing mechanisms are captured via the orientational elasticity term  $K(q') > 0$  and the viscous damping  $\eta(q') > 0$ . The  $a(q')$ -term represents the essence of the Carr-Helfrich destabilizing mechanism: The factor  $(\epsilon_a/\epsilon_\perp - \sigma_a/\sigma_\perp) < 0$  displays the charge separation effect coupled to the hydrodynamic torque contribution  $(\alpha_2 q'^2 - \alpha_3) < 0$ . The crucial difference in the threshold behavior between standard MBBA and MBBA\* with  $\epsilon_a > 0$  comes from the dielectric torque term  $(\epsilon_a/\epsilon_\perp)B(q')$ , which is only weakly frequency dependent. For  $\epsilon_a < 0$  this term is negative (stabilizing) with a minimum at  $q' = 0$ . The term  $q'^2 A(q')$  which has to compensate  $(\epsilon_a/\epsilon_\perp)B(q')$  ( $U_0^2 > 0$  is necessary for EC!), has a maximum for  $q' \sim 1.2$  for small frequencies that decreases with increasing  $\omega'$  and shifts to larger  $q'$ . Since minimization of  $U_0(q')$  requires, loosely speaking, maximization of the denominator in Eq. 6 the decrease of  $A(q')$  with increasing  $\omega'$  has to be balanced by larger  $q'_c$  values. In contrast, for  $\epsilon_a > 0$  the situation is just opposite, the contributions of  $q'^2 A(q')$  and  $(\epsilon_a/\epsilon_\perp)B(q')$  add up and  $q'_c(\omega')$  will in fact even decrease.

With the use of Eq. (6) the linear properties of electroconvection can be easily assessed for other material parameters as well. For instance the Fredericksz transition  $U_F$  would precede  $U_c$  for  $\epsilon_a \gtrsim 0.295$  for MBBA\* as already mentioned in [4]. In general one has also to be aware of a possible bifurcation to oblique rolls with the critical wave vector  $\mathbf{q}_c = (q_c, p_c)$  including a finite angle with the preferred direction  $\hat{\mathbf{x}}$  in the cell [4]. In this case the exact threshold behavior can also be described very well by a slightly more complicated one mode formula [4, 13], which contains Eq. (6) as a special case for  $p_c = 0$ . While the threshold voltage in the case of an oblique roll bifurcation is only slightly below the normal roll threshold according to Eq. (6) the roll angle  $\alpha = \arctan(p_c/q_c)$  is fairly sensitive against variations of the material parameters [4]. Finally we would like to mention that the convection regime can be enlarged with the use of a horizontal magnetic field [27]. The Fredericksz threshold according to  $U_F = \pi\sqrt{k_{11}/(\epsilon_0\epsilon_a)}\sqrt{1 + (H_x/H_F)^2}$  is then shifted to larger values, whereas  $U_c$  reacts less sensitively. For instance in the case of MBBA\* with  $\epsilon_a = 0.1$  and for  $H_x = H_F$  we find the values  $U_F = 12.19V$ ,  $U(0) = 6.26V$  such that the C2 point is shifted to the larger value  $\omega'_{C2} = 3.06$  (cf. Fig. 2a).

### B. Upper onset of convection at $U_c^F$

To calculate the upper onset of convection  $U_c^F$  a linear stability analysis of the the Fredericksz ground state  $\mathbf{V}_F = (\phi, \mathbf{n}_F, \mathbf{v} = 0)$  for  $U > U_F$  has been performed starting from Eq. (5) with the use of Galerkin methods.

It has turned out, that the general behavior of  $U_c^F$

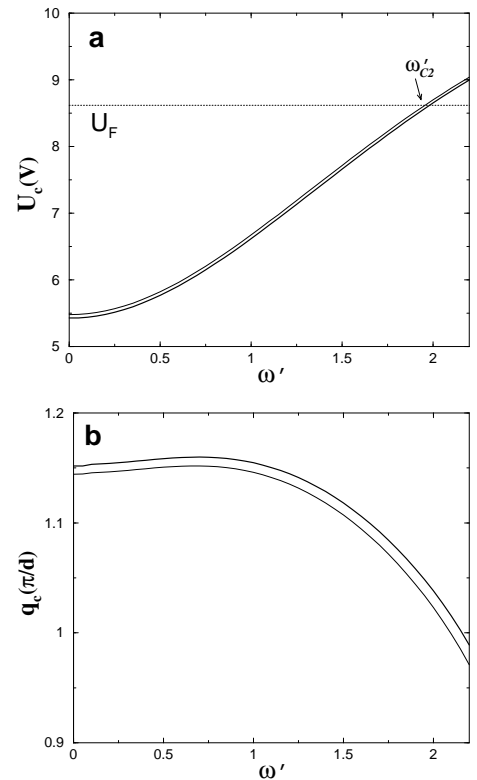


FIG. 2: Threshold voltage  $U_c$  (a) and critical wavenumber  $q_c$  in units of  $\pi/d$  (b) as function of the dimensionless frequency  $\omega'$  for MBBA\* with  $\epsilon_a = 0.1$  in comparison between rigorous numerical results (thick lines) and the analytical one-mode formula Eq. (6) (thin lines). The Fredericksz threshold  $U_F = \pi\sqrt{k_{11}/(\epsilon_a\epsilon_0)}$  is shown as well (a).

for  $\omega' \lesssim \omega'_{C2}$  can be satisfactorily described by an analytical approach, where only the leading Galerkin coefficients are kept. The Fredericksz solution, which bifurcates supercritically at  $U = U_F$  is calculated within a standard weakly nonlinear scheme. Near threshold the director reads  $\mathbf{n}_F = (1, 0, \psi_F \cos(\pi z/d))$  in the leading order of the amplitude  $\psi_F$ , which vanishes at  $U_F$ . To order  $O(\psi_F^3)$ , where the corrections  $\sim \psi_F^2$  to  $n_x = 1$  and  $\phi_0$  come into play, one arrives at a Landau-type equation  $\partial_t \psi_F = \sigma_S \psi_F - g_F \psi_F^3$  with the saturation coefficient  $g_F$  and the splay growth rate

$$\sigma_S = \tau_d \frac{\epsilon_a \epsilon_0 (U^2 - U_F^2)}{\gamma_1 d^2}. \quad (7)$$

The linear growthrate  $\sigma_S$  crosses zero at  $U_F$ ;  $\tau_d = \alpha_0 d^2 / (k_0 \pi^2)$  denotes the director relaxation time, where  $\alpha_0 = 10^{-3} Ns/m^2$  and  $k_0 = 10^{-12} N$  set the scales for the viscosity and elasticity effects, respectively.

The calculation of  $g_F$  is straightforward and the final expression for  $g_F^{-1}$  can be read off in the square bracket

of the following explicit representation:

$$\begin{aligned}\psi_F^2 &= \sigma_S \left[ \frac{2\gamma_1 d^2}{\tau_d \pi^2 (k_{33} - \frac{3}{4}k_{11} + C(U, \omega'))} \right] \\ &\equiv c_1 (U^2 - (U_F)^2); \\ C(U, \omega') &= \frac{U^2 \epsilon_a \epsilon_0}{\pi^2} \left( \frac{3}{4} + \frac{\sigma_a / \sigma_\perp + \omega'^2 \epsilon_a / \epsilon_\perp}{1 + \omega'^2} \right),\end{aligned}\quad (8)$$

which is valid in the limit  $U \rightarrow U_F, \omega' \rightarrow \omega'_{C2}$ .

In the next step the linear stability analysis of the Freedericksz solution has to be performed. For finite  $\psi_F$  the planar director symmetry is broken and the periodic director fluctuation crucial in the Helfrich mechanism to drive EC are impeded; consequently the threshold must increase compared to  $U_c$ . Technically one has to repeat the calculations that led to  $U_c$  (see Eq. (6)), but now for the nontrivial distorted ground state ( $\mathbf{n} = \mathbf{n}_F$ ). We will skip the straightforward though somewhat lengthy calculations. The final result in the vicinity of  $\omega'_{C2}$  becomes very transparent if written in the following form:  $(U_c^F)^2 - (U_c)^2 = c[(U_c^F)^2 - (U_F)^2] \propto \psi_F^2$ , consistent with  $U_c^F = U_c$  at  $\psi_F = 0$ . Solving for  $U_c^F$  we obtain:

$$(U_c^F)^2 = \frac{c(U_F)^2 - (U_c)^2}{c - 1}, \quad c = c_1 c_2 \quad (c > 1). \quad (9)$$

It turns out that the factor  $c_2$ , which has to be calculated numerically, depends mainly on some overlap integrals, while the material parameter dependence is condensed in the parameter  $c_1$  defined in Eq. (8). It is obvious from Eq. (9) that the line  $U_c^F$  starts at the C2 point ( $U_c = U_F$ ) as well. Furthermore, inspection of Eq. (8) proves that for fixed  $\epsilon_a, \sigma_a$  an increase of the bend constant  $k_{33}$  leads to a decrease of  $\psi_F$  and of  $c_1$ . Thus the slope of  $U_c^F(\omega')$  depends rather sensitively on  $k_{33}$ , which is for instance known to increase strongly with temperature near a nematic-smectic transition [28]. In Fig. 1 the analytical threshold curve  $U_c^F$  with  $c_1 \approx 0.019, c_2 \approx 97.8$  for MBBA\* ( $\epsilon_a = 0.1$ ) is compared with the rigorous numerical results. As to be expected from our weakly nonlinear approach there is in fact good agreement near the C2 point  $\omega'_{C2}$  where  $\psi_F$  is not too large.

#### IV. NONLINEAR REGIME

After the discussion of the linear threshold lines  $U_c, U_F$  and  $U_c^F$  in section III we will now turn to the phase diagram for the nonlinear states that bifurcate at these lines. Our numerically demanding analysis has focused on the interesting regime near  $\omega' = \omega'_{C2}$ , since for lower frequencies the well investigated familiar EC bifurcation scenarios for  $\epsilon_a < 0$  (see e.g. [24] were expected and indeed found in some selected test runs (for more details see [29])). The analysis of the periodic solutions and their stability is again based on Galerkin methods, by which Eq. (5) is mapped on a system of nonlinear algebraic equations for the expansion coefficients with respect to

suitable test functions. The equations are solved by a Newton iteration scheme and in general tested for stability with the use of the standard methods [13, 24].

In Fig. 3 the complete phase diagram in the  $U, \omega'$ -plane near the C2 point ( $\omega'_{C2} = 1.99$ ) is shown which is considered to be generic for EC instabilities in nematics with slightly positive  $\epsilon_a$ . Let us discuss at first the white wedged-shaped convection regime delineated by the lines  $U_c$  and  $U_c^F$ . Increasing the applied voltage at lower  $\omega'$  the normal rolls above  $U_c$  become at first unstable against the long-wavelength zig-zag (ZZ) instability, which involves undulations along the roll axis. At the line  $U_S$ , on the other hand, a homogeneous splay mode  $n_z^S = \psi_S \cos(\pi z/d)$  spontaneously bifurcates. For  $\omega'$  larger than the crossing point,  $\omega' = 1.75$ , of  $U_{ZZ}$  and  $U_S$ , the splay mode is directly superimposed onto the periodic director distortion with amplitude  $A$  leading to the so-called splay rolls [15] characterized by the off-plane director component  $n_z = (A \cos(qx) + \psi_S) \cos(\pi z/d)$ . The

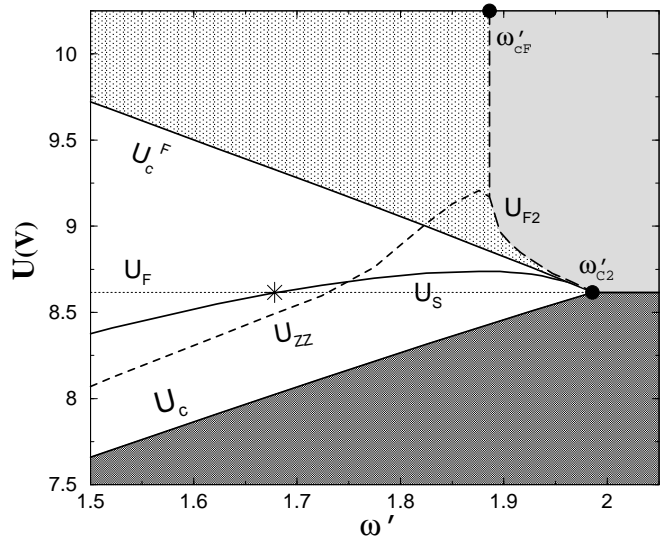


FIG. 3: Complete phase diagram for MBBA\* with  $\epsilon_a = 0.1$  for frequencies  $\omega'$  near the C2 point  $\omega'_{C2}$  (see text) on the basis of Galerkin calculations for rolls with the critical wavevector  $q_c(\omega')$ . The bifurcation lines above onset ( $U_c$ ) indicate the zig-zag instability ( $U_{ZZ}$ ), the Freedericksz transition ( $U_F$ ), the splay-roll bifurcation ( $U_S$ ), the Freedericksz  $\rightarrow$  convection ( $U_c^F$ ) and the convection  $\rightarrow$  Freedericksz transition ( $U_{F2}$ ).

bifurcation at  $U_S$  in Fig. 3 is supercritical and can appear above or below the (in the convection regime,  $\omega' < \omega'_{C2}$ , irrelevant) line  $U_F$ . Although the transition is certainly favored by the dielectric torque for  $\epsilon_a > 0$  it is also driven by complex nonlinear interactions between the director and the flow field. In fact splay rolls have been identified and discussed also in buoyancy driven thermal convection in nematics [15].

The interaction between the convection-mode amplitude  $A$  and the homogeneous splay director distortion  $\psi_S$  is captured by coupled order parameter equations for

$A$  and  $\psi_S$ :

$$\begin{aligned}\partial_t A &= (\sigma_R - g_R |A|^2 - \beta \psi_S^2) A, \\ \partial_t \psi_S &= (\sigma_S + \Gamma_\psi |A|^2) \psi_S.\end{aligned}\quad (10)$$

All coefficients have been calculated and good agreement with the Galerkin analysis has been found. For  $\psi_S = 0$  the  $A$ -equation describes the supercritical bifurcation of the rolls with the amplitude  $A^2 = \sigma_R/g_R \propto U^2/U_c^2 - 1$  at  $U_c$ . The splay-roll bifurcation takes place, when the effective growth rate  $\sigma_S^{eff} = \sigma_S + \Gamma_\psi A^2$  becomes larger than zero. The coefficient  $\Gamma_\psi$  is negative for smaller  $\omega'$  before it changes sign at  $\omega' < \omega'_S = 1.68$ , marked by a star in Fig. 3. The form of  $U_S(\omega')$  can be understood on the basis of Eq. (10): In the regime  $\omega' < \omega'_S$  a splay bifurcation at  $U_S < U_F$  is possible, because the contribution  $\Gamma_\psi A^2 > 0$  in  $\sigma_S^{eff}$  can compensate  $\sigma_S$ , which is negative for  $U < U_F$  (cf. Eq. (7)). For  $\omega' > \omega'_S$  the negative  $\Gamma_\psi$  term suppresses at first the positive  $\sigma_S$  term in  $\sigma_S^{eff}$  resulting in  $U_S > U_F$ .

Of particular interest is the upper bifurcation line  $U_c^F$  (see also Eq. (9) and Fig. 1), at which the Fredericksz state becomes convectionally unstable when *lowering* the voltage from above. A weakly-nonlinear-expansion at the line  $U_c^F$  with respect to the convective perturbation yields a negative saturation coefficient  $g$  for frequencies  $\omega' < \omega'_{C2}$  in the resulting Landau equation, indicating a subcritical bifurcation.  $g$  is strongly decreasing with frequency, i.e. the subcritical nature becomes more pronounced at lower  $\omega'$ . However, it should be emphasized that the line  $U_c^F$  has in principle no relevance, when the voltage is *increased* from below, i.e. when starting from convective Galerkin solutions inside the white wedged-shaped regime in Fig. 3. In fact, we found these solutions to exist far beyond  $U_c^F$  in the nonlinear regime, but we were not able to study systematically their stability. Only in an intermediate frequency range  $\omega'_{cF} < \omega' < \omega'_{C2}$  above (and on the right of) the line  $U_{F2}$  in Fig. 3 convection ceased to exist. Thus, in contrast to the unique Fredericksz-solution in the bright grey region, *bistability* exists between the Fredericksz- and convective solutions in the grey-shaded area enclosed between  $U_c^F$  and  $U_{F2}$ .

For a better illustration of the subcritical nature of the convection onset at  $U_c^F$  and the interplay between the Fredericksz state and convection, it is useful to follow the order parameters  $A$  and  $\psi$  (obtained as Galerkin solutions), when the reduced control parameter  $\epsilon = U^2/U_c^2 - 1$  is continuously increased at fixed  $\omega'$ . The case  $\omega' = 1.88$  slightly below  $\omega'_{cF} = 1.89$  is shown in Fig. 4a. At first the amplitude  $A$  (solid line) of the periodic roll state grows  $\propto \sqrt{\epsilon}$  above  $\epsilon = 0$  in line with the supercritical bifurcation at  $U_c$ . At  $\epsilon_S$  the homogeneous splay mode  $\psi_S$  (dot-dashed line) bifurcates. Though a further increase in  $A$  is then slowed down, splay-roll convection solution continue to exist up to large  $\epsilon$ , as already mentioned. On the other hand we have learnt from our previous considerations in section III B, that a pure Fredericksz state  $\psi_F$  with  $A = 0$ , which bifurcates at  $\epsilon_F$ ,

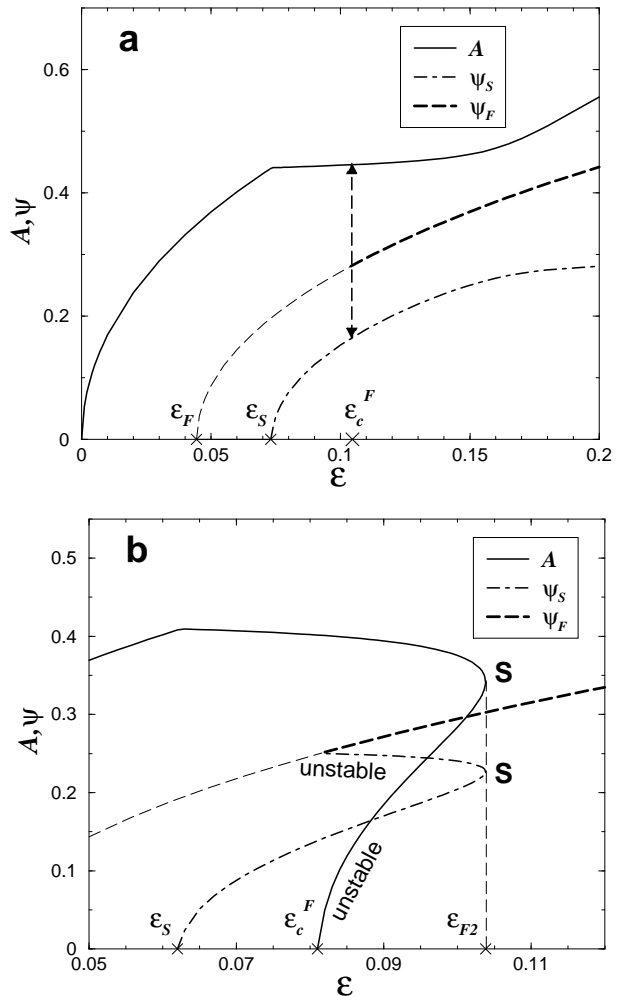


FIG. 4: Amplitudes for the off-plane director-distortion  $n_z = (A \cos(q_c x) + \psi_S + \psi_F) \cos(\pi z/d)$  as function of the reduced control parameter  $\epsilon = U^2/U_c^2 - 1$  for frequencies slightly below/above the transition frequency  $\omega'_{cF} = 1.89$  at  $\omega' = 1.88$  (a) and  $\omega' = 1.90$  (b).  $A$  describes the periodic off-plane director excursions in convection rolls and  $\psi_S$ ,  $\psi_F$  the homogeneous splay distortion in the convection or Fredericksz state, respectively. For a detailed explanation, see text.

can exist only for  $\epsilon > \epsilon_c^F = (U_c^F)^2/U_c^2 - 1$  (thick dashed line). Thus decreasing  $\epsilon$  in the Fredericksz state from above leads in any case at  $\epsilon = \epsilon_c^F$  to a discontinuous jump (indicated by the double-arrows in Fig. 4a) from the Fredericksz solution  $n_z^F = \psi_F \cos(\pi z/d)$  (Eq. (8)) to the splay rolls (Eq. (10)) with  $A, \psi_S \neq 0$ . Obviously, for  $\epsilon > \epsilon_c^F$  we recover the bistability between convection and the Fredericksz state.

The situation changes for frequencies  $\omega' > \omega'_{cF}$  since the bistable regime is restricted to an  $\epsilon$ -range between  $\epsilon_c^F$  and  $\epsilon_{F2}$  in Fig. 4b. Above  $\epsilon_{F2} \simeq 0.105$  only the Fredericksz solution exists ( $A = 0, \psi = \psi_F$ ). As demonstrated in Fig. 4b the point  $\epsilon = \epsilon_{F2}$  corresponds then to the saddle node (S) of the backward bifurcation at

$\epsilon_c^F$ , which connects the stable and unstable branches of the roll- and splay mode  $A$ ,  $\psi_S$ , respectively. At  $\epsilon_c^F$  the splay amplitude branch  $\psi_S$  and the Freedericksz solution  $\psi_F$  have to merge in line with Fig. 4b. The upper solid  $A$ -line in Fig. 4b, which approaches zero at  $\epsilon = 0$  (not shown) corresponds to the  $A$ -line in Fig. 4a. In the same manner  $\psi_F$  (dashed) approaches zero at  $\epsilon_F$ , as shown in Fig. 4a. When approaching  $\omega'_{cF}$  from above, the saddle node moves obviously to large  $\epsilon$  along the almost vertical separation line  $U_{F2}$  for  $\omega' = \omega'_{cF}$  in Fig. 3. Note that the unstable solutions starting at  $\epsilon_c^F$  in Fig. 4b have not vanished; only for clarity they are suppressed in Fig. 4a, because they have no physical relevance.

## V. CONCLUSION

In conclusion we have demonstrated that planar nematics with slightly positive  $\epsilon_a$  (and positive  $\sigma_a$ ) show interesting nonlinear EC states which result from the competition between a convection-mode and homogeneous splay mode. Above the subcritical transition  $U_c^F$  from the Freedericksz into convection state a bistability

between a Freedericksz solution (equilibrium state) and convective solution (non-equilibrium state) was clearly identified. A transition frequency  $\omega_{cF}$  could be determined below which we have been able to construct splay roll solutions up to high voltages, whereas for  $\omega > \omega_{cF}$  with increasing voltage a discontinuous transition to a Freedericksz state occurs. The bifurcation diagrams are believed to display the generic features. Support stems from the detailed physical interpretation of the destabilization mechanism as well as from the observation that parameter modifications led only to some quantitative changes. We hope that our comprehensive theoretical analysis will motivate new experimental studies. Besides a careful exploration of the linear destabilization lines  $U_c$ ,  $U_c^F$  and the C2 point, the investigation of the bistable regime above  $U_c$  looks promising. One might for instance achieve a better insight into the nature of inhomogeneous Freedericksz states in the presence of walls between symmetry degenerated configurations  $\pm\psi_F$  where according to Eq. (2) also a flow is excited.

We would like to thank I. Rehberg, T. Bock and L. Kramer for useful discussions.

- 
- [1] M.C. Cross and P.C. Hohenberg, *Rev. Mod. Phys.* **65**, 851 (1993).
- [2] P.G. de Gennes, *The Physics of Liquid Crystals* (Clarendon Press, Oxford, 1974).
- [3] S. Kai and W. Zimmermann, *Prog. Theor. Phys. Suppl.* **99**, 458 (1989).
- [4] E. Bodenschatz, W. Zimmermann, and L. Kramer, *J. Phys. (Paris)* **49**, 1875 (1988).
- [5] L. Kramer and W. Pesch, *Annu. Rev. Fluid Mech.* **27**, 515 (1995).
- [6] F. C. Frank, *Disc. Far. Soc.* **25**, 19 (1958).
- [7] H. Richter, A. Buka, and I. Rehberg, in *Spatio-Temporal Patterns in Nonequilibrium Complex Systems*, edited by P.E. Cladis and P. Palfy-Muhoray (Addison-Wesley, New York, 1995).
- [8] J.-H. Huh, Y. Hidaka, and S. Kai, *Phys. Rev. E* **58**, 7355 (1998).
- [9] W. Pesch and U. Behn, in *Evolution of Spontaneous Structures in Dissipative Continuous Systems*, edited by F.H. Busse and S.C. Müller (Springer, Berlin, 1998).
- [10] L. Kramer, B. Dressel, H. Zhao, and W. Pesch, *Mol. Cryst. Liq. Cryst.* **364**, 101 (2000).
- [11] J.T. Gleeson, *Nature* **256**, 511 (1996).
- [12] See e.g. G.H. Heilmeyer, L.A. Zannoni, and L.A. Barton, *Proceedings of the IEEE* **56**, 1162 (1968); B.J. Lechner, F.J. Marlowe, and E.O. Nester, *ibid.* **59**, 1566 (1971).
- [13] L. Kramer and W. Pesch, in *Pattern Formation in Liquid Crystals*, edited by A. Buka and L. Kramer (Springer, New York, 1996).
- [14] E. Plaut, W. Decker, A.G. Rossberg, L. Kramer, W. Pesch, A. Belaidi, and R. Ribotta, *Phys. Rev. Lett.* **79**, 2367 (1997).
- [15] B. Dressel, A. Joets, L. Pastur, W. Pesch, E. Plaut, and R. Ribotta, *Phys. Rev. Lett.* **88**, 024503 (2002).
- [16] H. Richter, N. Klöpper, A. Hertrich, and A. Buka, *Europhys. Lett.* **30**, 37 (1995).
- [17] W.H. de Jeu, C.J. Gerritsma, and T. Lathouwers, *Chem. Phys. Lett.* **14**, 5031 (1972).
- [18] M.I. Barnik, L.M. Blinov, M.F. Grebenki, S.A. Pikin, and V.G. Chigrinov, *Phys. Lett. A* **51**, 175 (1975).
- [19] P.R. Kishore, *Mol. Cryst. Liq. Cryst.* **128**, 75 (1985); P.R. Kishore, T.F.S. Raj, A.W. Iqbal, S.S. Sastry, and G. Satyanandam, *Liquid Crystals* **14**, 1319 (1993).
- [20] The material parameter set MBBA I in [4] is used except that  $\epsilon_a$  is allowed to vary. In line with [4] the average dielectric constant  $\bar{\epsilon} = (2\epsilon_{\perp} + \epsilon_{\parallel})/3$  is fixed for convenience to the pure MBBA value  $\bar{\epsilon} = 5.07$ .
- [21] The molecular structure of the large- $\epsilon_a$  materials like EBCA (4-ethoxybenzylidene-4'-cyanoaniline) differs mainly by substituting the butyl-group in MBBA (4-methoxybenzylidene-4'-n-butylaniline) by the strongly polarizable cyano group. In the mixture MBBA-EBCA the resulting value  $\epsilon_a$  varies linearly with the concentration of EBCA; for instance  $\epsilon_a = 0.1$  corresponds to a concentration of  $\approx 2.3\%$  (weight percentage) [19]. Thus it is not surprising that MBBA\* with the material parameters of pure MBBA, except  $\epsilon_a$ , describe well the experiments.
- [22] E.F. Carr, *Mol. Cryst. Liq. Cryst.* **7**, 253 (1969).
- [23] W. Helfrich, *J. Chem. Phys.* **51**, 4092 (1969).
- [24] E. Plaut and W. Pesch, *Phys. Rev. E* **59**, 1747 (1998).
- [25] F.M. Leslie, *Quart. J. Mech. appl. Math.* **19**, 357 (1966).
- [26] Although depending on the choice of certain test functions previous one-mode formulas to be found in the literature [4, 13] look slightly different, their results match practically with Eq. (6). Note that the threshold  $U_0$  (Eq. (6)) depends only on the ratios of the viscosity coefficients  $\alpha_i$  ( $i = 1, \dots, 6$ ), which fulfill the Parodi relation  $\alpha_2 + \alpha_3 = \alpha_6 - \alpha_5$ . According to the definition of the

Miesowicz coefficient  $\eta_1, \eta_2$  (see paragraph after Eq. (2)) only the sum  $\alpha_4 + \alpha_5$  enters, such that in fact only *three* independent combinations of the  $\alpha_i$  are relevant. In addition from measurements of  $U_F = \sqrt{k_{11}/(\epsilon_a \epsilon_0)}$ , of the codimension-2 point  $\omega_{C2}$  in units of  $\tau_q = (\epsilon_\perp \epsilon_0)/\sigma_\perp$  and of  $U_0(\omega)$  one gets further valuable informations to asses the parameters.

[27] The theoretical analysis in [19], based on an old analytical threshold formula (E. Dubois-Violette, P.G. de Gennes,

and O. Parodi, J. Phys. (Paris) **32**, 305 (1971)), is only useful to reproduce qualitative trends in the dependence on the material parameters. In contrast to Eq. (6) one finds considerable quantitative deviations from the rigorous numerical results.

[28] F. Jähnig and F. Brochard, J. Phys. (Paris) **35**, 301 (1974).

[29] B. Dressel, PhD thesis, Bayreuth 2002.